



RESEARCH MEMORANDUM

FREE-FLIGHT ROLL PERFORMANCE OF A STEADY-FLOW JET-SPOILER
CONTROL ON AN 80° DELTA-WING MISSILE BETWEEN
MACH NUMBERS OF 0.6 AND 1.8

By Eugene D. Schult

Langley Aeronautical Laboratory
Langley Field, Va.

NATIONAL ADVISORY COMMITTEE
FOR AERONAUTICS

WASHINGTON
January 24, 1958
Declassified March 18, 1960

NATIONAL ADVISORY COMMITTEE FOR AERONAUTICS

RESEARCH MEMORANDUM

FREE-FLIGHT ROLL PERFORMANCE OF A STEADY-FLOW JET-SPOILER
CONTROL ON AN 80° DELTA-WING MISSILE BETWEEN
MACH NUMBERS OF 0.6 AND 1.8

By Eugene D. Schult

SUMMARY

A free-flight investigation of the zero-lift control effectiveness of a steady-flow jet-spoiler roll control was conducted on a cruciform 80° delta-wing missile between Mach numbers of 0.6 and 1.8. Measurements were made of rolling-moment, damping-in-roll derivative, drag, and pressures at the inlet and on the wing near the jet exit as the control was pulsed to alternate positions. Jet air was supplied by two tip-mounted normal-shock inlets of one-fifth fuselage diameter.

The results demonstrated that the wing and jet combination magnified the thrust force of the isolated jet alone by factors of 11 at subsonic speeds to 3 at supersonic speeds. Both the control rolling-moment coefficients and the wing or jet back-pressure coefficients associated with spoiling approached a constant at supersonic speeds. The rolling power of the test control compared favorably with conventional ailerons, each deflected 5°, and the incremental drag is attributed primarily to the presence of the inlet stores.

INTRODUCTION

The current interest in jet spoilers for missiles originates from a need for a simple control having low actuating forces and possible application at altitudes both within and beyond the atmosphere.

Recent studies on controls have established that the primary jet-control force at high altitudes (reaction) may be considerably augmented at lower altitudes by combining the jet and wing in a manner to alter or "spoil" the main flow over the wing. Previous tests show, for example, that the total control force obtained from inlet-supplied jets favorably located at the trailing edge and blowing approximately normal to the surface exceeds the pure reaction component by a factor of approximately

10 at subsonic speeds and 3 at supersonic speeds (refs. 1 and 2). These same tests also reveal that forward jet locations tend to produce control reversals similar to those experienced by common plate spoilers at forward positions and low projections.

The use of inlets as the jet energy source is based primarily on simplicity and weight considerations at low and medium altitudes. The use of the gas generator as an alternative jet energy source would appear, on the basis of rough calculations, to be limited to high-altitude missions where its fuel requirements are less severe. Needless to say, the inlet design is also important when optimum pressure recovery, drag, and range are considerations.

For a given inlet size the control effectiveness of an inlet-jet spoiler combination has been found to vary nonlinearly with orifice area (ref. 3). This nonlinearity becomes more pronounced with increased ratio of orifice to inlet areas and, as might be expected, is caused primarily by internal flow losses which increase with increased flow rate. A proposed solution is to employ a steady-flow system which exhausts the air continually to both upper and lower surfaces in proportions depending upon the desired control sense. Conceivably then since the flow rate remains essentially constant for given flight conditions, the flow requirements of this system could be matched with that of the inlet to minimize inlet spillage and possibly reduce the inlet drag. Of general interest in this connection is a knowledge of the jet-induced wing pressures or jet back pressures associated with aerodynamic spoiling.

The present paper presents the results of free-flight tests of a steady-flow jet-spoiler control which provided roll at zero lift for an 80° delta cruciform missile configuration at Mach numbers between 0.6 and 1.8. Air for the trailing-edge jet was obtained from a simple normal-shock inlet. The test measurements of control effectiveness, jet-induced wing pressures, and drag were obtained as the control was pulsed to alternate positions. The merit of the wing-jet combination is judged by comparing its effectiveness with that of pure reaction for the jet alone exhausting to the free stream and also with that of conventional ailerons.

The flight test was conducted at the Langley Pilotless Aircraft Research Station at Wallops Island, Va.

SYMBOLS

A_i	projected intake frontal area, sq ft unless noted otherwise
A_j	jet exit area, sq ft unless noted otherwise
b	total wing span, ft
C_D	total drag coefficient of configuration, $\frac{\text{Drag}}{qS_{\text{exposed}}}$
C_l	rolling-moment coefficient, $\frac{\text{Rolling moment}}{qSb}$
$C_{l,j}$	total rolling-moment coefficient due to jet-spoiler control
C_{l_0}	rolling-moment coefficient due to constructional asymmetries
C_{l_p}	damping-in-roll derivative, $\frac{\partial C_l}{\partial \left(\frac{pb}{2V} \right)}$
C_F	jet-thrust coefficient, $\frac{F}{(P_t - P_a)A_j}$
c_p	specific heat at constant pressure
c_v	specific heat at constant volume
K_F	force magnification produced by wing-jet combination relative to reaction force alone of isolated jet exhausting to free-stream conditions
F	pure jet-reaction force component normal to wing chord plane, lb
I_X	mass moment of inertia of model about longitudinal axis, slug-ft ²
I_Y, I_Z	mass moments of inertia of model in the pitch and yaw planes, respectively, about axes through the center of gravity, slug-ft ²

y_j	jet-reaction-force control-moment arm; spanwise ordinate from plane of symmetry to midcontrol span, ft
M	Mach number
p	model rolling velocity, radians/sec
\dot{p}	model roll acceleration, $\frac{dp}{dt}$, radians/sec ²
$p_b/2V$	wing-tip helix angle, radians
P_t	total pressure measured at center of inlet face, lb/sq ft
P_a	local static or jet back pressure on wing surface near jet exit, lb/sq ft
P_∞	static pressure of free stream, lb/sq ft
q	dynamic pressure of free stream, $\frac{\gamma}{2} P_\infty M^2$, lb/sq ft
R	Reynolds number based on a length of 1 foot
S	total cruciform wing area projected to fuselage center line, sq ft
t	time, sec
V	model forward velocity, ft/sec
δ_V	deflection of jet-control valve from neutral control position, positive for increased jet-flow rate from upper surface of right wing, deg
γ	ratio of specific heats, $\frac{c_p}{c_v}$, 1.40 for air
(S_f/S_e)	ratio of exposed flap-control area to exposed wing area for one wing panel

MODEL AND INSTRUMENTATION

Dimensions and photographs of the flight test model are presented in figures 1 and 2. The 80° delta cruciform wings had modified hexagonal

sections with blunt trailing edges equal to one-half maximum thickness. A small portion of the wing leading edge near the body juncture was removed for structural reasons and rounded off in such a manner that the 0.06-inch leading-edge radius was maintained. The wings were constructed of 1/4-inch-thick aluminum-alloy plate cycle welded to mahogany overlays. The fuselage was constructed of an aluminum-alloy cylinder joined to a 3.5-fineness-ratio plastic nose containing an NACA 4-channel telemeter. Two steel inlet-jet-spoiler assemblies were embedded in opposite wing panels. The ratios of inlet-to-fuselage diameter and inlet-to-jet-orifice area were arbitrarily 1/5 and 3/2, respectively. No attempt was made to match the inlet with jet-flow requirements. The control-valve spindles were machined from 1/4-inch steel rod with flats at intervals corresponding to the orifice slots. During flight a 33-rpm motor and a 4-link mechanism cycled the valves in a sinusoidal manner between opposite control positions.

Model instrumentation consisted of a roll accelerometer, an inductance-type valve-position pickup, and two pressure cells to record on one wing the stream total pressure at the inlet station and the local wing static pressure at a position just forward of the jet at midcontrol span. All pressure probes and lines were 3/32-inch outside (1/16-inch inside) diameter. The exposed mounting arrangement of the wing static-pressure probe (fig. 2(b)) was necessary because of space limitations between the manifold and wing surface; one orifice was drilled on each side of this probe at a position 1.5 probe diameters forward of the probe end and 2 diameters forward of the jet slot.

PREFLIGHT TESTS

Blowing tests of the two jet-spoiler manifold assemblies were conducted individually at several levels of inlet total pressure to measure the variation of jet thrust with control-valve displacement and to ascertain the actual neutral control positions. Air from a compressed-air tank was supplied to the manifold assembly through, respectively, a throttling valve, a straight flexible duct, a screened settling chamber, and an inlet bell attached to and faired in smoothly with the inlet face. The measured thrust was the effective roll-producing force component normal to the wing chord plane. The inlet total pressure was measured at the center of inlet station zero by means of the same probe employed for the flight tests. The ambient pressure at the jet exit was atmospheric.

The physical characteristics of the model and the possible sources of roll asymmetry were also evaluated prior to the flight tests. Measurements of the wing and inlet incidence indicated that the wing contribution was 0.03° of clockwise roll-causing incidence. By comparison, the inlet contributions were negligible.

FLIGHT TESTS

A single-stage ABL deacon rocket motor accelerated the combination to the maximum test Mach number in about 3 seconds and then separated from the model. All test measurements were made within the following 20 seconds of flight along the ascending portion of the model trajectory. In addition to the telemeter information described previously, time histories were obtained of the forward velocity and space coordinates by using a CW Doppler velocimeter and an NACA modified SCR-584 radar set. These measurements and rawinsonde data permitted an evaluation of Mach number, Reynolds number, dynamic pressure, and total-drag coefficient. Measurements of the model rolling velocity were determined by means of spinsonde rotating-antenna ground receiving equipment which monitored the radiated signal pattern of the model telemeter (ref. 4). The test Reynolds number variation with Mach number is shown in figure 3.

ACCURACY

The flight measurements are believed to be accurate to within the following limits:

M	±0.010
C_D	±0.002
p, radians/sec	±1.0
p, radians/sec ²	±2.5
P_t , lb/sq in.	±1.0
P_a , lb/sq in.	±0.4
P_∞ , lb/sq in.	±0.1
q, lb/sq in.	±0.3
δ_V , deg	±1.0

No determinations of the accuracy of the coefficients $C_{l,j}$ and $C_{l,p}$ were made. Because these two values were obtained from roll measurements in both directions, it is believed that the repeatability and scatter of test points for a complete control pulsing cycle constitutes in itself a fair indication of the data coefficient accuracy.

RESULTS AND DISCUSSION

The results of the present test are summarized in figures 4 to 13, inclusive.

Preflight Tests

Jet-thrust coefficients.- Figure 4(a) presents the thrust characteristics of the isolated jet as obtained from preflight blowing tests of the jet-spoiler control. The thrust measurements of the component of reaction force normal to the wing-chord plane were obtained as a function of valve displacement at arbitrary levels of inlet total pressure. The resulting curves are seen to be slightly nonlinear and reveal regions of thrust hysteresis which are attributed primarily to viscous effects associated with the current valve design. Mechanical hysteresis due to valve friction acting on the slender valve spindle may also have been a contributing factor. It was noted, however, that the hysteresis abruptly terminated at valve positions where the jet was observed to change abruptly in direction from a line parallel to the forward slot lip to one parallel to the spindle face. (See inset in fig. 4(a).) These nonlinear and hysteretic effects are reflected to some extent in the flight-test results which follow, and consequently an improved valve design, as suggested later in the paper, is recommended for future application. The valve-actuating torque was not measured during these tests, although it was observed to be small and only slightly greater than the air-off friction torque.

In figure 4(b) the preceding measurements of jet reaction are reduced to thrust coefficients in a form suitable for application to free-flight conditions. (See appendix.) These results are compared with estimates based on one-dimensional theory for convergent nozzles (ref. 1). The isentropic curve represents coefficients obtained by assuming an ideal flow expansion through the nozzle from uniform upstream stagnation conditions at the inlet. For convenience, the jet of the theoretical model is directed normal to the wing-chord plane rather than slightly off-normal as in the actual case. Since this small angularity introduces little error, it is evident that the large thrust loss for the actual model occurred as a result of large flow losses through the manifold and orifice. According to previous data, these losses could be reduced substantially by straightening the internal flow path (ref. 1). Shown also in figure 4(b) is a curve of the estimated pressure ratios necessary for choking the orifice when the thrust coefficients are reduced below the isentropic value because of internal losses.

Flight Tests

A time history of the significant model measurements taken during flight for a complete control pulse cycle is presented in figure 5. The method of reducing these data to obtain the rolling-moment coefficient of the control and the damping-in-roll derivative is outlined in the appendix.

Jet-spoiler-control effectiveness.- Variations of the total rolling-moment coefficient of the jet spoiler with control-valve deflection are presented in figure 6 for Mach numbers between approximately 0.6 and 1.8. Arbitrary curves faired through the data points for each control pulse cycle demonstrate that the rolling moments varied linearly with valve deflection up to near the maximum deflection. Further increases in deflection generally resulted in progressively less effectiveness. Contributing to this nonlinearity, however, is the valve overlap shown in figure 5. There appears to be little effect of Mach number or helix angle on the jet effectiveness over the range of Mach numbers or roll rates encountered during a cycle (figs. 5 and 6).

Figure 7(a) presents the variation with Mach number of the initial slopes of the rolling-moment coefficients per degree of control deflection. The results indicate that the jet-spoiler effectiveness approaches a constant at supersonic speeds. In figure 7(b) the maximum jet-spoiler effectiveness is compared with the thrust reaction alone of the isolated jet as derived from preflight thrust data (see appendix). The ratio of values from these curves at a given Mach number are the force magnifications, K_F in the insets, which are gained from the wing-jet combination. These magnifications varied between 11 at subsonic speeds to 3 at supersonic speeds and are in good agreement with those obtained in previous tests (refs. 1 and 2). On the basis of data presented later, it is quite possible that the actual thrust-force contribution is less than the thrust shown for the isolated jet because of the higher jet back pressure associated with spoiling. With this added consideration one might expect the spoiling-force component to continue as the primary control force for inlet-jet spoilers at higher Mach numbers.

The above thrust gains due to spoiling will probably change if higher-energy jet sources than the free stream are employed. For the high altitude control problem, it may be of interest, therefore, to review the general effect on spoiler performance of increasing the relative jet energy level or the "effective spoiler height" as indicated by the jet momentum coefficient, $2(q_j/q)(A_j/S)$, or more directly by the ratio of jet-to-free stream dynamic pressure. Recent low-speed tests (ref. 5) indicate that as this ratio is increased from zero, the induced spoiling-force increment is characterized by a rapid initial increase followed by a gradual approach to some constant which is related to and may exceed the aerodynamic lift of the basic wing. Since the jet thrust increases in proportion to pressure ratio, the spoiling force eventually becomes small by comparison so that K_F approaches unity as a limit. Thus, when constant-output, high-energy, jet sources are used, one might expect K_F to vary considerably with Mach number and altitude and the limit condition to be reached quite easily at extreme altitudes. By comparison, inlet-supplied jets would tend to have less variation in K_F with Mach number and little effect of altitude. Some loss in K_F as a result of increased orifice opening, (A_j/S) , or "jet thickness" is also indicated by tests of throttled-orifice inlet flows (ref. 1).

A comparison of the rolling power of the inlet jet spoiler with conventional flap-type and detached-surface ailerons is illustrated in figure 8. As with the present jet control, the ailerons (ref. 1) are attached to two of the four wing panels and the ailerons are arbitrarily deflected 5° each or 10° differentially. The wings were identical except for the sharp trailing edges used in connection with the narrow-chord flap and detached surface configurations. In general, it appears that the present jet spoiler has a rolling effectiveness equivalent to 10-percent area-ratio flaps, each deflected 5°, and the spoiler retains its effectiveness to higher Mach numbers.

Pressure coefficients.- Samples of the local wing static pressure just forward of the jet at midcontrol span and the inlet total pressure were obtained during the flight. The static-pressure results for the wing upper surface are presented in figure 9 as coefficients plotted against control-valve deflection for several control pulses. These pressures varied, as might be expected, between a negative limit established by the wing section without the jet to a maximum positive pressure corresponding to the intensity of wing-flow jet interaction (aero-dynamic spoiling). The consistency of the data obtained over a complete control cycle reveals that the differences in Mach number or local helix angle due to roll encountered during a given pulse cycle had little effect on the coefficients except near sonic speeds.

The relationship between the local wing pressures and the rolling moments to which they contribute can be illustrated by reflecting the measured curve about $\delta_y = 0$ in order to represent the static wing pressures on the opposite surface (fig. 10). The curve representing the difference between upper- and lower-surface pressures is observed to be more nonlinear than the corresponding rolling-moment coefficient curve for this pulse in figure 6(b). This fact seems to indicate that the wing area affected by the jet-induced pressure field is increasing with increased jet-flow rate.

The effect of Mach number on the maximum level of this local-pressure field is presented in figure 11 together with total-pressure measurements taken at the inlet station. The results show that at supersonic speeds, Mach number has little influence on the pressure coefficients associated with jet spoiling. The effect of Mach number on the maximum extent of this pressure field is difficult to determine from the limited information obtained; however, on the basis of the leveling trends in both the preceding pressure data and the rolling-moment data of figure 7, there are indications that the maximum area of this pressure field probably also approaches a constant for this configuration at supersonic speeds.

The observed trend toward constant jet-induced wing pressure coefficients forward of the jet at supersonic speeds is contrary to results obtained for rigid spoilers of fixed height for which the coefficients

decrease with increased Mach number (refs. 6 and 7). This difference may be caused by the rising inlet total-pressure coefficient with increased Mach number which would increase the so-called "effective height" of the jet spoiler with increased Mach number.

The broken curves in figure 11 are obtained from estimates derived in the appendix for the effective jet total pressure available after manifold and orifice losses and for the maximum back pressure (Pa)_{crit.} for choked orifice conditions. In view of the apparent pressure losses sustained by the present manifold configuration, it is felt that an effort to improve the inlet and manifold design would substantially improve the total-pressure recovery and control effectiveness at high Mach numbers. Oblique-shock or spiked inlets and a less torturous flow path may be rewarding in this respect. A comparison of the measured jet back pressures with those estimated to obtain choking indicates that the jets remained subsonic throughout most of the test speed range. For this condition the positive back pressures induced by the jet produced not only a force amplification but also tended to reduce the actual jet-flow rate below that required for the same jet when isolated from the wing and considered as a simple reaction device.

Damping-in-roll derivative.- Results of C_{l_p} are plotted against Mach number for the test configuration in figure 12. These points are in good agreement with values interpolated from data of reference 8 for other flight models with delta cruciform wings swept back 45° , 60° , and 70° , respectively. Cross plots of C_{l_p} against sweep angle, made under the assumption that $C_{l_p} = 0$ at 90° sweep, yield the comparative points shown. The slender-body theory of reference 9 overestimated experimental data approximately 15 percent.

Drag coefficient.- Figure 13 presents a measured drag breakdown of the test configuration. The peaks in the oscillations of the curve for drag coefficient with Mach number coincided with the peaks in the curve for rolling velocity (see fig. 5). In contrast to the drag resulting from rigid spoilers, it is believed that the drag resulting from the jet spoiler or from the wing pressures induced by the jet is relatively small. The reasons for this belief are based on the lack of a drag-producing step, the negative slope of the wing profile near the jet exit, and the possible alleviation of negative wing base pressures as a result of jet flow. Moreover, an estimate from reference 10 of the drag coefficient of two solid blunt-nose stores outwardly similar to the inlets is of the order of the indicated drag increment at supersonic speeds. The major portion of the drag of the control is therefore attributed to the normal-shock inlets and to the inlet spillage resulting from the large ratio of intake to orifice areas (1.50).

Suggested control redesign for future study or application.- The preceding results have indicated that modifications in the test-control system might improve the control effectiveness and possibly reduce the inlet drag at high speeds. These modifications deal with the design of the jet-control valve to eliminate hysteresis, with a manifold duct design to provide essentially straight flow paths between inlet and orifice, and with a matched inlet design to improve total-pressure recovery and reduce drag at high Mach numbers. Figure 14 illustrates a possible trend in redesign. The original lip design, which contributed to flow hysteresis, is eliminated in the suggested valve. The suggested valve design is also believed to be more suitable than the original from the standpoint of simplicity and wing thickness required as well as being less likely to seize at the temperatures encountered at high Mach numbers.

CONCLUSIONS

A free-flight investigation of the zero-lift control effectiveness of a steady-flow, inlet-jet-spoiler roll control was conducted on a cruciform 80° delta-wing missile between Mach numbers of 0.6 and 1.8. An analysis of the roll response and measured pressures obtained while the control was pulsed to alternate control positions indicated the following conclusions:

1. The control effectiveness of the air-jet spoiler varied linearly with jet-control valve deflection up to near the maximum deflection. Further increases in deflection generally resulted in progressively less effectiveness.
2. The wing and jet in combination magnified the thrust force of the isolated jet alone by a factor of 11 at subsonic speeds to 3 at supersonic speeds.
3. Both the rolling-moment coefficients and the wing pressure coefficients associated with jet spoiling approached a constant at supersonic speeds.
4. The rolling effectiveness of the air-jet spoiler compared favorably with that of 10-percent area ratio, plain flap-type ailerons, each deflected 5° . At supersonic speeds the rolling effectiveness of the jet spoiler approached a constant level in contrast to that obtained with the deflected-surface type of controls.

5. The drag of the control is attributed primarily to the presence of the inlet stores.

Langley Aeronautical Laboratory,
National Advisory Committee for Aeronautics,
Langley Field, Va., October 1, 1957.

APPENDIX

DATA REDUCTION AND ANALYSIS

Rolling-Moment Data

The total rolling-moment coefficients for the jet spoiler $C_{l,j}$ and the model damping-in-roll derivative $C_{l,p}$ were obtained from the flight data by using the following first-order differential equation which describes the pure rolling motion of the model for any jet-control valve position:

$$\frac{I_X \dot{p}}{qSb} - C_{l,p} \left(\frac{b}{2V} \right) p = C_{l,j} + C_{l_o} \quad (A1)$$

Here C_{l_o} is the rolling-moment coefficient due to roll-causing construction asymmetries. On the present model the primary asymmetry was differential wing incidence ($i_W = 0.03^\circ$) which is an ever-present and essentially steady-state component; therefore, C_{l_o} may be approximated by the following steady-state relation:

$$\frac{p_o b}{2V} = \frac{C_{l_o}}{-C_{l,p}} \quad (A2)$$

Here p_o is the roll-rate contribution due to wing incidence. Solving for C_{l_o} and substituting in equation (A1) yields:

$$\frac{I_X \dot{p}}{qSb} - C_{l,p} \left(\frac{b}{2V} \right) (p - p_o) = C_{l,j} \quad (A3)$$

For the present model configuration p_o is of the following order (from ref. 1):

$$p_o \approx (0.0285) (i_W) (V) \approx 0.001V$$

or less than 2 radians per second during the flight.

A general solution of equation (A3) for the unknowns C_{l_p} and $C_{l,j}$ was not considered practical because of the nonharmonic nature of the control input and the nonlinearity of $C_{l,j}$ with control-valve position. Instead, a method of successive approximations was employed which determined the coefficients directly from equation (A3) in two steps. It was assumed that the damping derivative is independent of the rolling velocity and that, for purposes of a first approximation, $C_{l,j} = 0$ when $\delta_V = 0$. Under these assumptions initial values of C_{l_p} were determined at discrete time intervals during the flight history when $\delta_V = 0$. These C_{l_p} data were plotted against Mach number, and points obtained from a faired curve were substituted into equation (A3) to give preliminary values of $C_{l,j}$ throughout the flight history. Plots of $C_{l,j}$ against δ_V yielded values of δ_V where $C_{l,j} = 0$. A second calculation of C_{l_p} at conditions where $C_{l,j} = 0$ then gave new values of the damping derivative (fig. 12) which essentially reproduced the original faired curve with less scatter. Small readjustments in $C_{l,j}$ were made accordingly in order to obtain the results presented herein (fig. 6). Additional readjustments had a negligible effect on the final coefficients.

Jet-Reaction Data

The preflight measurements of the maximum jet-reaction-force component normal to the wing chord plane were reduced to thrust coefficients (fig. 4(b)) by means of the following relation from reference 3.

$$C_F = \frac{F}{(P_t - P_a)A_j} \quad (A4)$$

where P_t is the upstream total pressure measured at the inlet station and P_a the ambient pressure to which the jet exhausts. In contrast to other expressions for the thrust coefficient which contain q or simply P_t , equation (A4) is probably more convenient for applying preflight thrust measurements to the flight situation since it provides for variations in the local wing or jet back pressure which may arise from differences in wing section, altitude, and angle of attack, or as a result of spoiling.

The maximum rolling-moment coefficient due to the reaction alone of the isolated jet control exhausting to free-stream conditions was determined from the relation:

$$\begin{aligned}
 C_l &= C_F \left(\frac{P_t - P_\infty}{q} \right) \left(\frac{A_j}{S} \right) \left(\frac{y_j}{b} \right) \\
 &= C_F \left(\frac{2}{\gamma M^2} \right) \left(\frac{P_t}{P_\infty} - 1 \right) \left(\frac{A_j}{S} \right) \left(\frac{y_j}{b} \right)
 \end{aligned} \tag{A5}$$

by using measured values of the total pressure ratio (P_t/P_∞), the total jet-exit area of two controls for A_j , and the total area of four wing panels for S .

Ideal Jet-Thrust Coefficients

The ideal coefficients for isentropic flow expansion from the inlet station through the manifold and orifice were derived in reference 1 and are given here for convenience. The thrust vector is assumed to coincide with the nozzle axis of symmetry.

$$\begin{aligned}
 \text{For subsonic orifices } &\left(P_t/P_a \leq \left(\frac{\gamma + 1}{2} \right)^{\frac{\gamma}{\gamma-1}} \text{ or } \leq 1.89 \text{ for air} \right): \\
 C_{F_{\text{ideal}}} &= \frac{2 \left(\frac{\gamma}{\gamma - 1} \right) \left[\left(P_t/P_a \right)^{\frac{\gamma-1}{\gamma}} - 1 \right]}{\left(P_t/P_a \right) - 1} \\
 &= 7 \left[\frac{\left(P_t/P_a \right)^{0.286} - 1}{\left(P_t/P_a \right) - 1} \right]
 \end{aligned} \tag{A6}$$

where $\gamma = 1.40$ for air.

$$\begin{aligned}
 \text{For critical flow or choked orifices } &\left(P_t/P_a \geq \left(\frac{\gamma + 1}{2} \right)^{\frac{\gamma}{\gamma-1}} \text{ or } \right. \\
 &\left. \geq 1.89 \text{ for air} \right):
 \end{aligned}$$

$$\begin{aligned}
 C_{F\text{ideal}} &= \frac{2\left(\frac{2}{\gamma+1}\right)^{\frac{1}{\gamma-1}}\left(P_t/P_a\right) - 1}{\left(P_t/P_a\right) - 1} \\
 &= \frac{1.27\left(P_t/P_a\right) - 1}{\left(P_t/P_a\right) - 1} \tag{A7}
 \end{aligned}$$

where $\gamma = 1.40$ for air. A curve of $C_{F\text{ideal}}$ against pressure ratio is plotted in figure 4(b) for comparison with actual thrust coefficients.

Effective Jet-Total-Pressure Ratio

An estimate may be made by means of equations (A6) and (A7) of the effective total pressure of the jet after upstream losses. In deriving the equations for the ideal C_F , it is noted that the pressure ratio in the denominator in both cases corresponds to that imposed across the system and may therefore be defined as a reference total-pressure ratio. The pressure term in the numerators, on the other hand, depends on the nature of the flow expansion through the nozzle and can be described as an effective total-pressure ratio available after manifold and orifice flow losses for producing the measured thrust-force component. If the expansion is ideal ($C_F = C_{F\text{ideal}}$) no losses would occur, and the total pressure would remain constant through the system and equal to the reference total pressure as expected. When the expansion is less than ideal ($C_F < C_{F\text{ideal}}$) the effective total pressure would be less than the reference by a factor depending on the losses incurred. By this reasoning, equations (A6) and (A7) may be rewritten as follows to obtain expressions for the actual C_F :

For subsonic orifices $\left(\left(P_t/P_a\right)_e \leq 1.89 \text{ for air}\right)$:

$$C_F = 7 \left[\frac{\left(P_t/P_a\right)_e^{0.286} - 1}{\left(P_t/P_a\right)_r - 1} \right] \tag{A8}$$

For choked orifices $\left(\left(P_t/P_a\right)_e > 1.89 \text{ for air}\right)$:

$$C_F = \frac{1.27 \left(P_t / P_a \right)_e - 1}{\left(P_t / P_a \right)_r - 1} \quad (A9)$$

where the subscripts e and r refer to the effective and reference pressure ratios, respectively.

In figure 11 the curve for the effective total-pressure coefficient of the jet was calculated by substituting into equations (A8) and (A9) the preflight measurements of C_F at the appropriate reference pressure ratios, solving for $\left(P_t / P_a \right)_e$ by letting $P_a = P_\infty$, and then converting this ratio to coefficient form. Neglected in these calculations is the small error associated with the inclination of the jet relative to a normal to the wing chord plane which in this case tends to underestimate slightly both C_F and the effective total pressure. Also neglected is the possible difference in distribution of flow through an open inlet compared to that obtained in the ground tests described previously. The resulting difference in thrust coefficient attributed to these sources is believed to be relatively small.

Critical Pressure Ratio With Upstream Losses

The upstream pressure in excess of the isentropic critical pressure necessary to choke the orifices for the conditions when $C_F < C_{F\text{ideal}}$ may be estimated either from equation (A8) or (A9). Substitution of

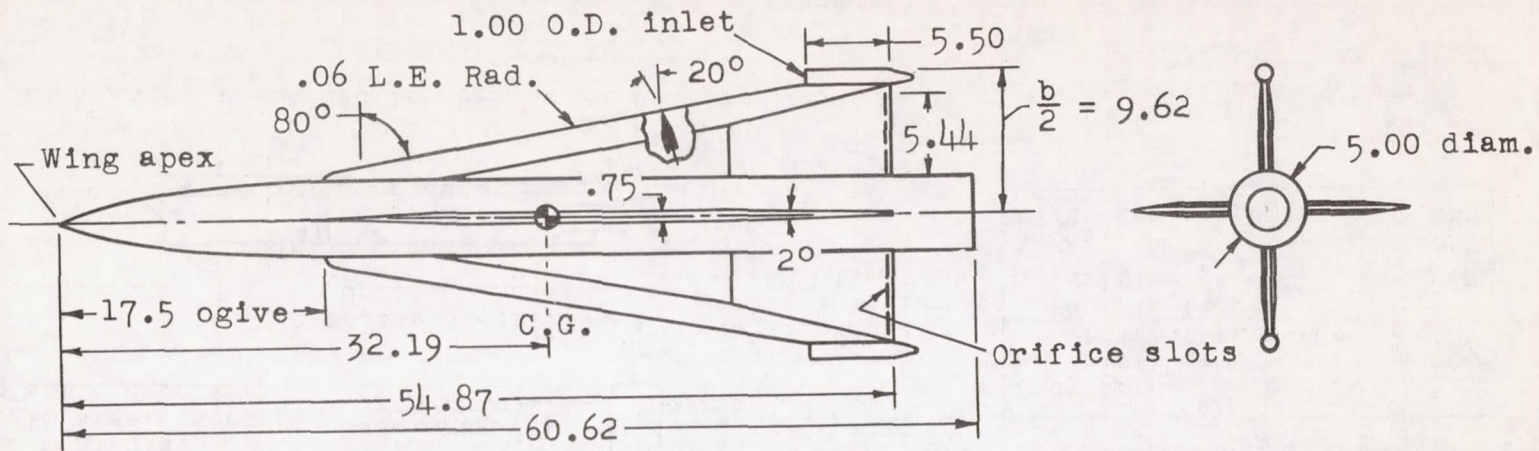
the critical pressure ratio $\left(P_t / P_a \right)_e = \left(\frac{\gamma + 1}{2} \right)^{\frac{\gamma}{\gamma-1}} = 1.89$ yields the following expression for the reference pressure ratio required for choking in terms of the actual C_F :

$$\begin{aligned} \left(P_t / P_a \right)_r &= \left(1 + \frac{\gamma}{C_F} \right) \\ &= \left(1 + \frac{1.40}{C_F} \right) \quad \text{for air} \end{aligned} \quad (A10)$$

This boundary is plotted in figure 4(b).

REFERENCES

1. Schult, Eugene D.: Free-Flight Investigation at Mach Numbers Between 0.5 and 1.7 of the Zero-Lift Rolling Effectiveness and Drag of Various Surface, Spoiler, and Jet Controls on an 80° Delta-Wing Missile. NACA RM L56H29, 1956.
2. Kehlet, Alan B.: Free-Flight Investigation of Comparative Zero-Lift Rolling Effectiveness of a Leading-Edge and a Trailing-Edge Air-Jet Spoiler on an Unswept Wing. NACA RM L57F10, 1957.
3. Schult, Eugene D.: A Free-Flight Investigation at High Subsonic and Low Supersonic Speeds of the Rolling Effectiveness and Drag of Three Spoiler Controls Having Potentially Low Actuating-Force Requirements. NACA RM L55G11a, 1955.
4. Harris, Orville R.: Determination of the Rate of Roll of Pilotless Aircraft Research Models by Means of Polarized Radio Waves. NACA TN 2023, 1950.
5. Lockwood, Vernard E., Turner, Thomas R., and Riebe, John M.: Wind-Tunnel Investigation of Jet-Augmented Flaps on a Rectangular Wing to High Momentum Coefficients. NACA TN 3865, 1956.
6. Lord, Douglas R., and Czarnecki, K. R.: Aerodynamic Loadings Associated With Swept and Unswept Spoilers on a Flat Plate at Mach Numbers of 1.61 and 2.01. NACA RM L55L12, 1956.
7. Lord, Douglas R., and Czarnecki, K. R.: Pressure Distributions and Aerodynamic Characteristics of Several Spoiler-Type Controls on a Trapezoidal Wing at Mach Numbers of 1.61 and 2.01. NACA RM L56E22, 1956.
8. Sanders, E. Claude, Jr.: Damping in Roll of Models With 45°, 60°, and 70° Delta Wings Determined at High Subsonic, Transonic, and Supersonic Speeds With Rocket-Powered Models. NACA RM L52D22a, 1952.
9. Adams, Gaynor J., and Dugan, Duane W.: Theoretical Damping in Roll and Rolling Moment Due to Differential Wing Incidence for Slender Cruciform Wings and Wing-Body Combinations. NACA Rep. 1088, 1952.
10. Hoerner, Sighard F.: Aerodynamic Drag. Publ. by the author (148 Busteed, Midland Park, N. J.), 1951.

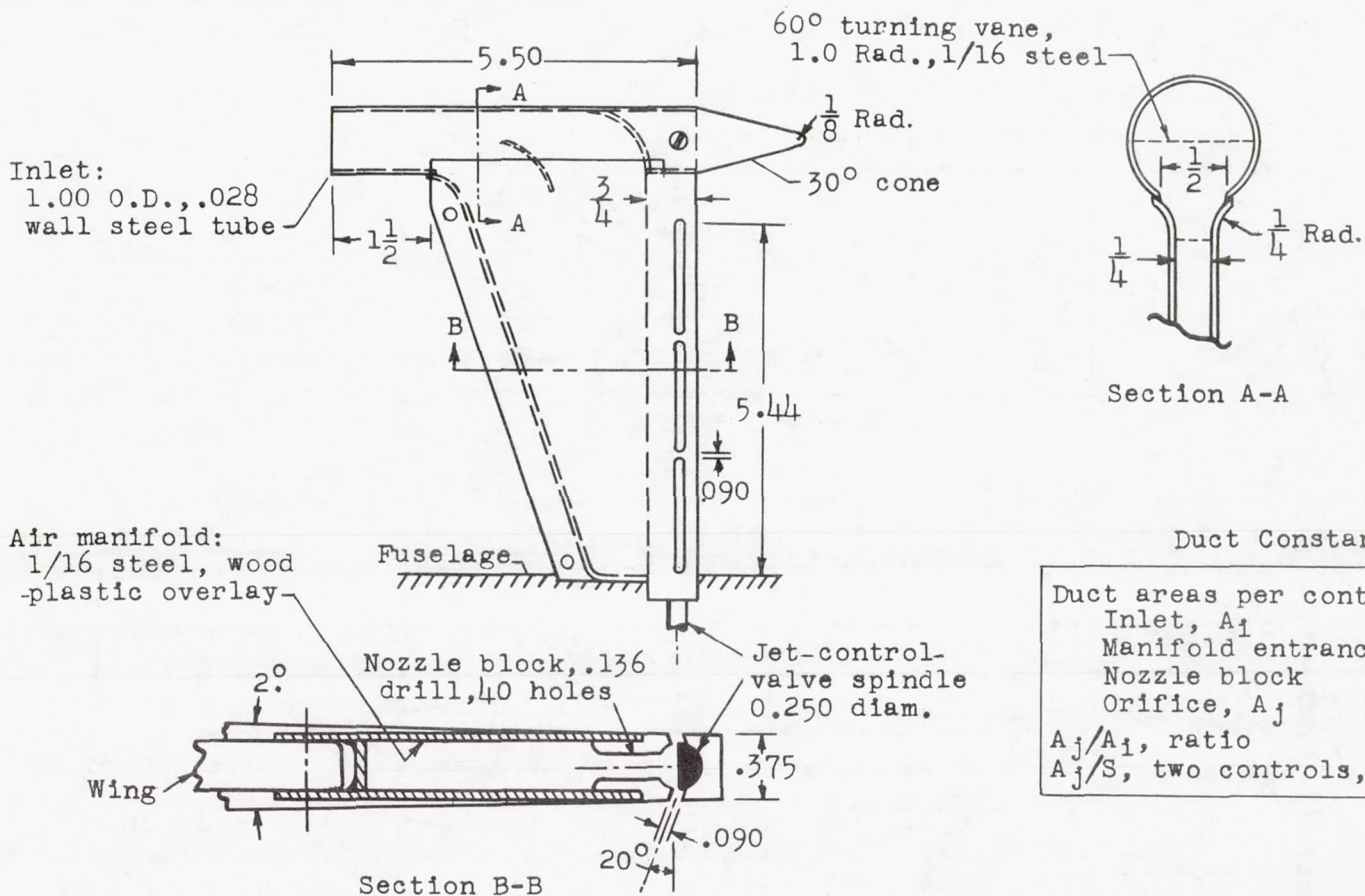


Model Constants

Wing aspect ratio	0.70
Total wing area, ft ²	7.29
Exposed wing area, ft ²	4.00
I_x (roll), slug-ft ²	0.13
I_y , I_z , slug-ft ²	3.10
Weight, lbs	61.00

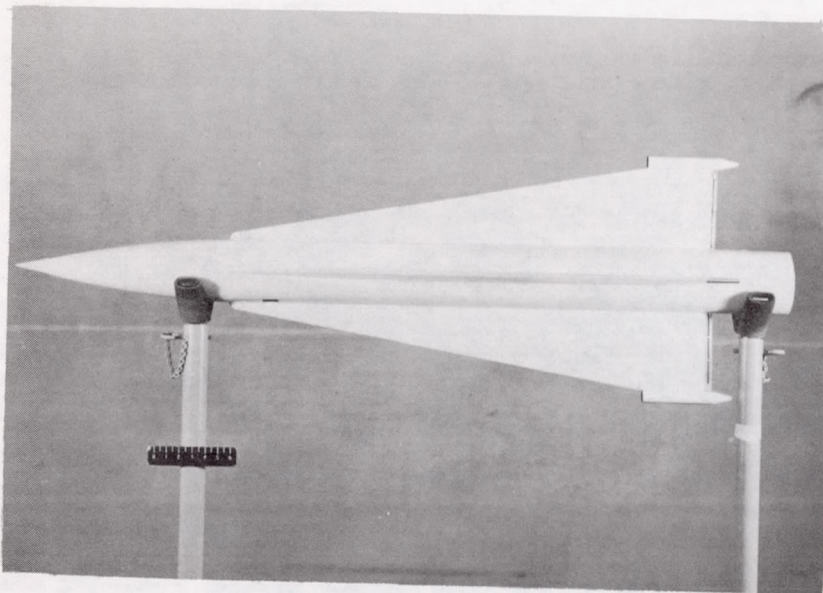
(a) Details of model.

Figure 1.- Details of model and jet control. Dimensions in inches unless otherwise noted.

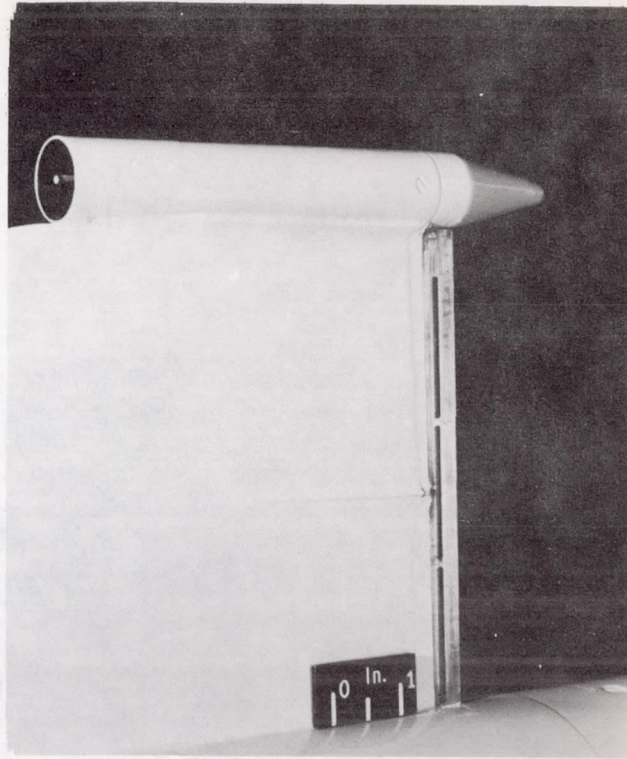


(b) Details of jet control.

Figure 1.- Concluded.

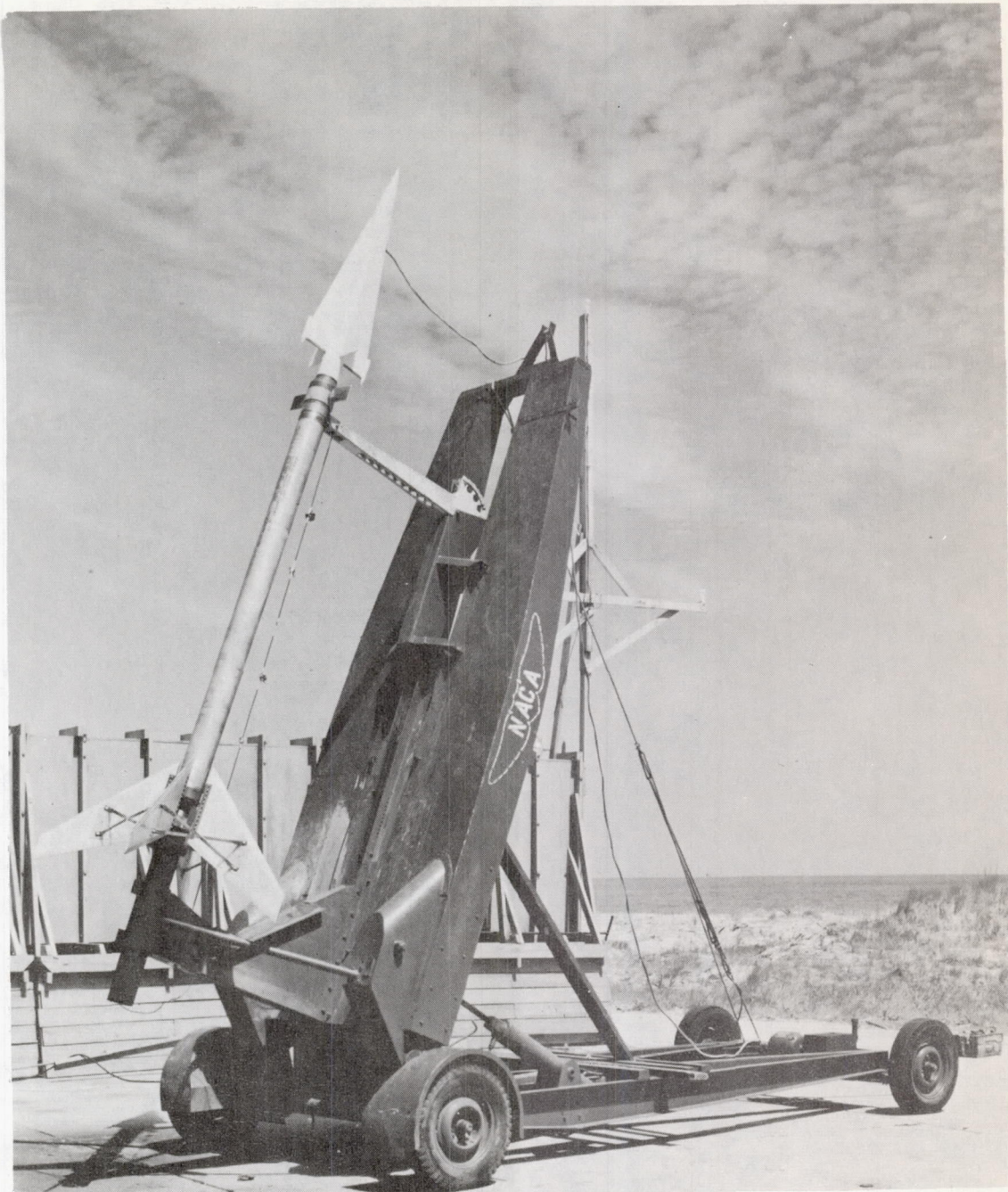


(a) Flight model.



(b) Closeup view of control. L-57-2774

Figure 2.- Photographs of test vehicle.



(c) Model and booster on launcher.

L-89539.1

Figure 2.- Concluded.

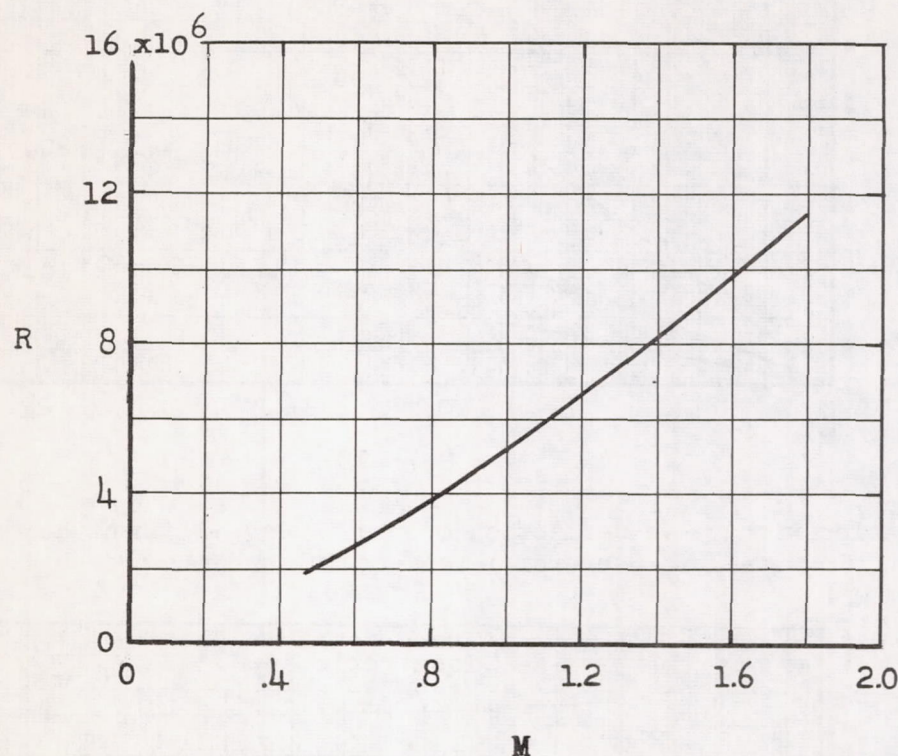
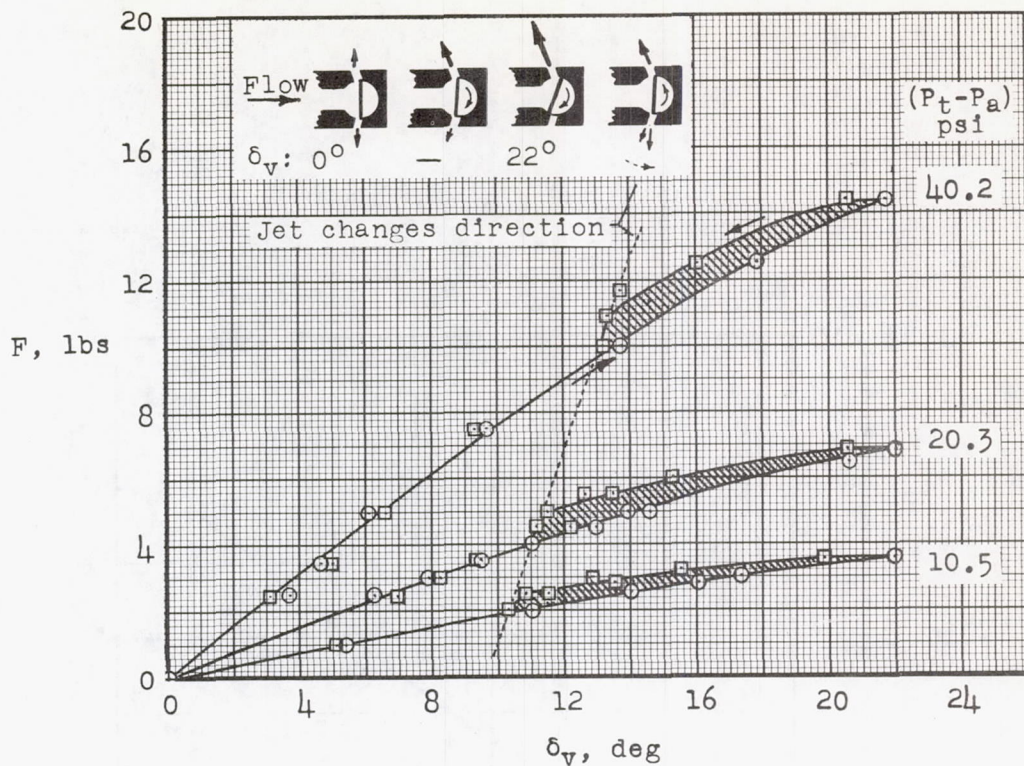
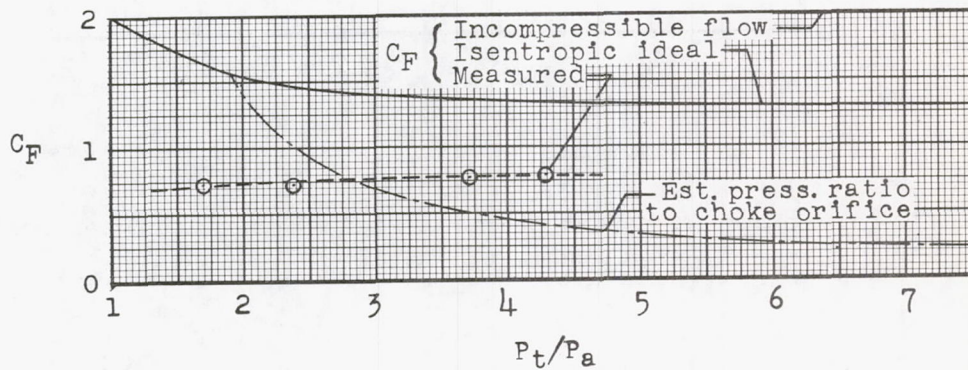


Figure 3.- Variation with Mach number of test Reynolds number based on a length of one foot.



- (a) Variation with valve deflection of the thrust component normal to each wing panel for several levels of inlet total pressure.



- (b) Thrust coefficients at maximum deflection compared with convergent nozzle theory.

Figure 4.- Thrust characteristics of jet spoiler based on preflight tests of the inlet-manifold-orifice combination. $A_j = 0.467$ sq in.; $A_j/A_1 = 0.67$; $P_a = P_\infty$.

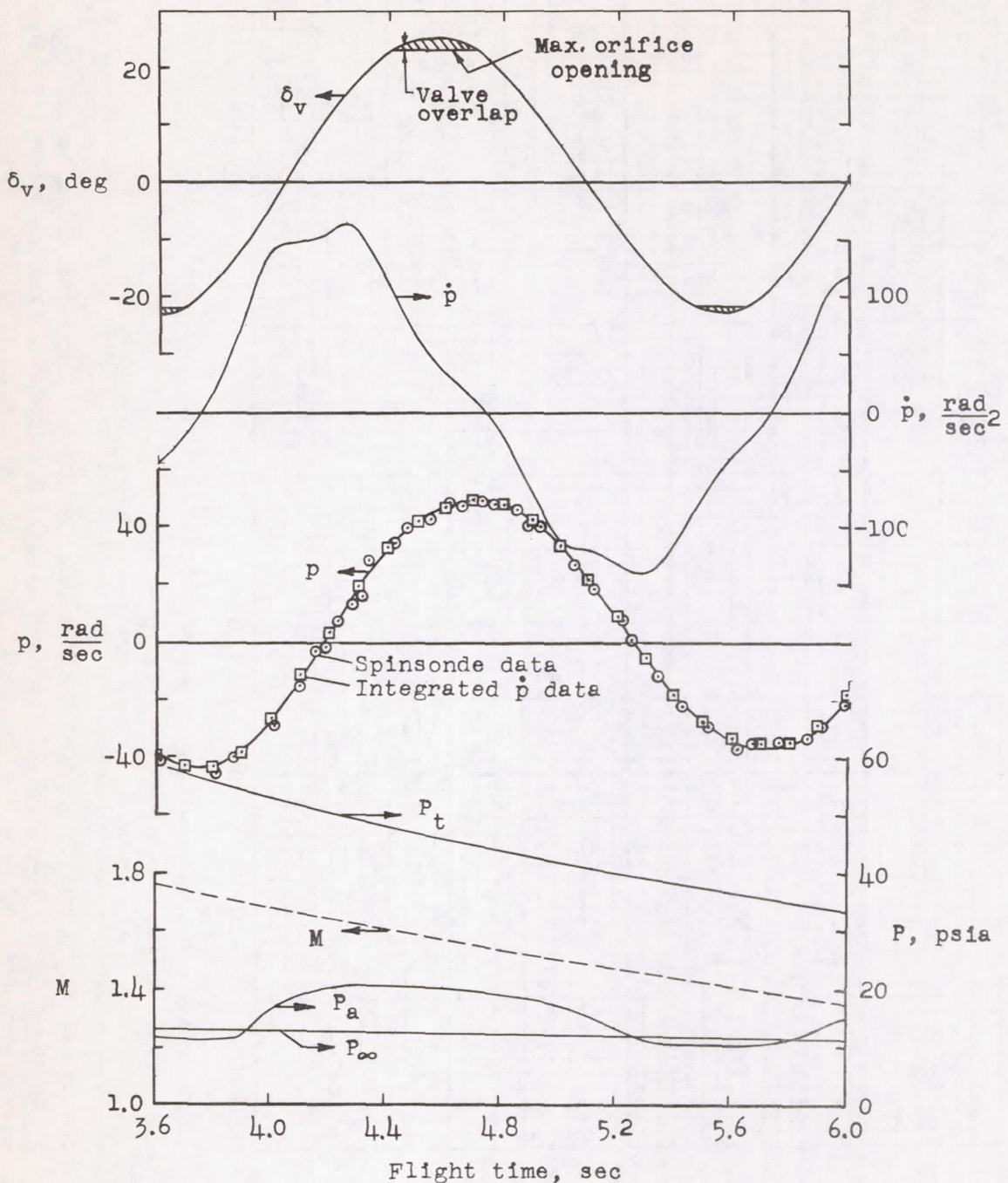
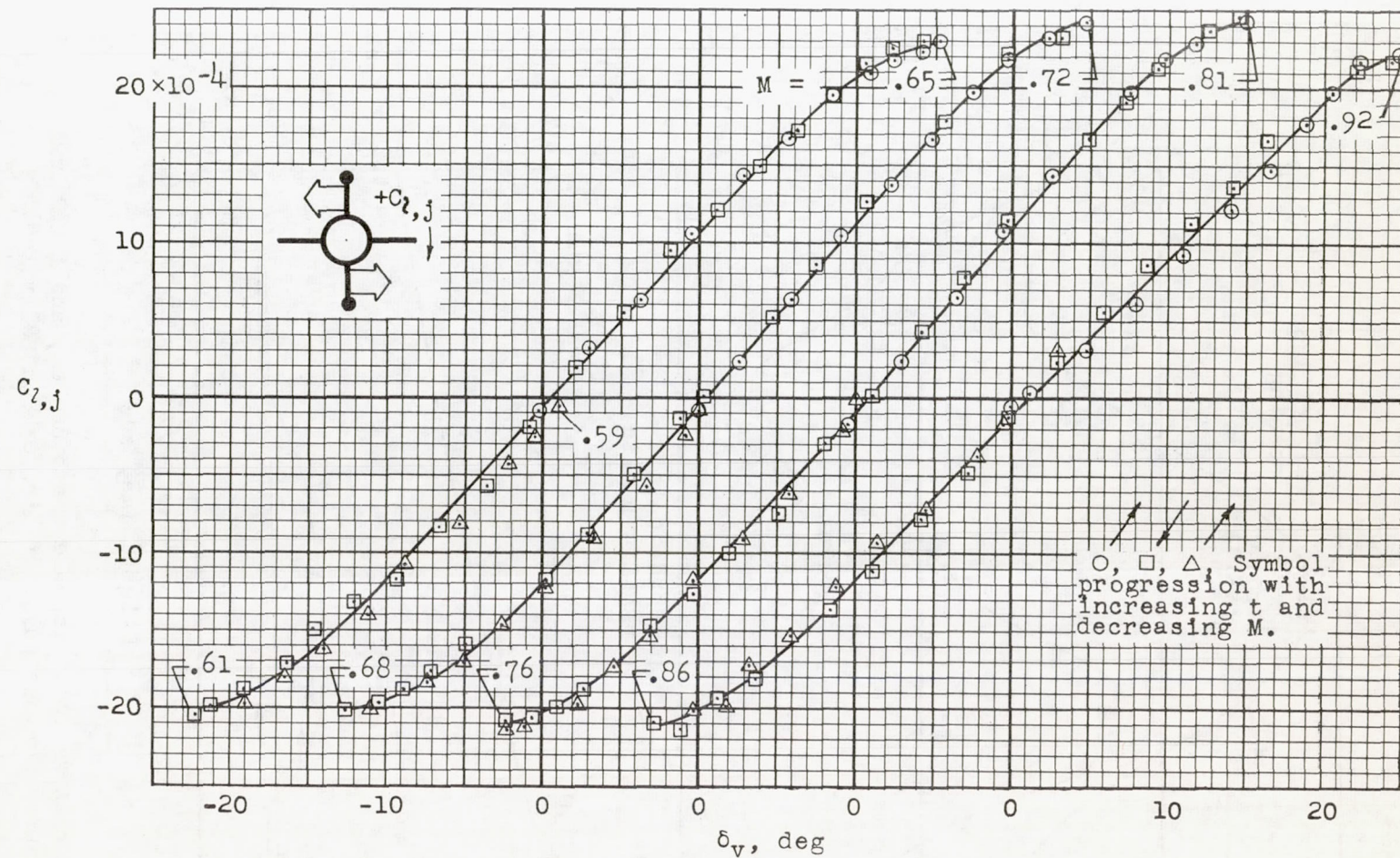
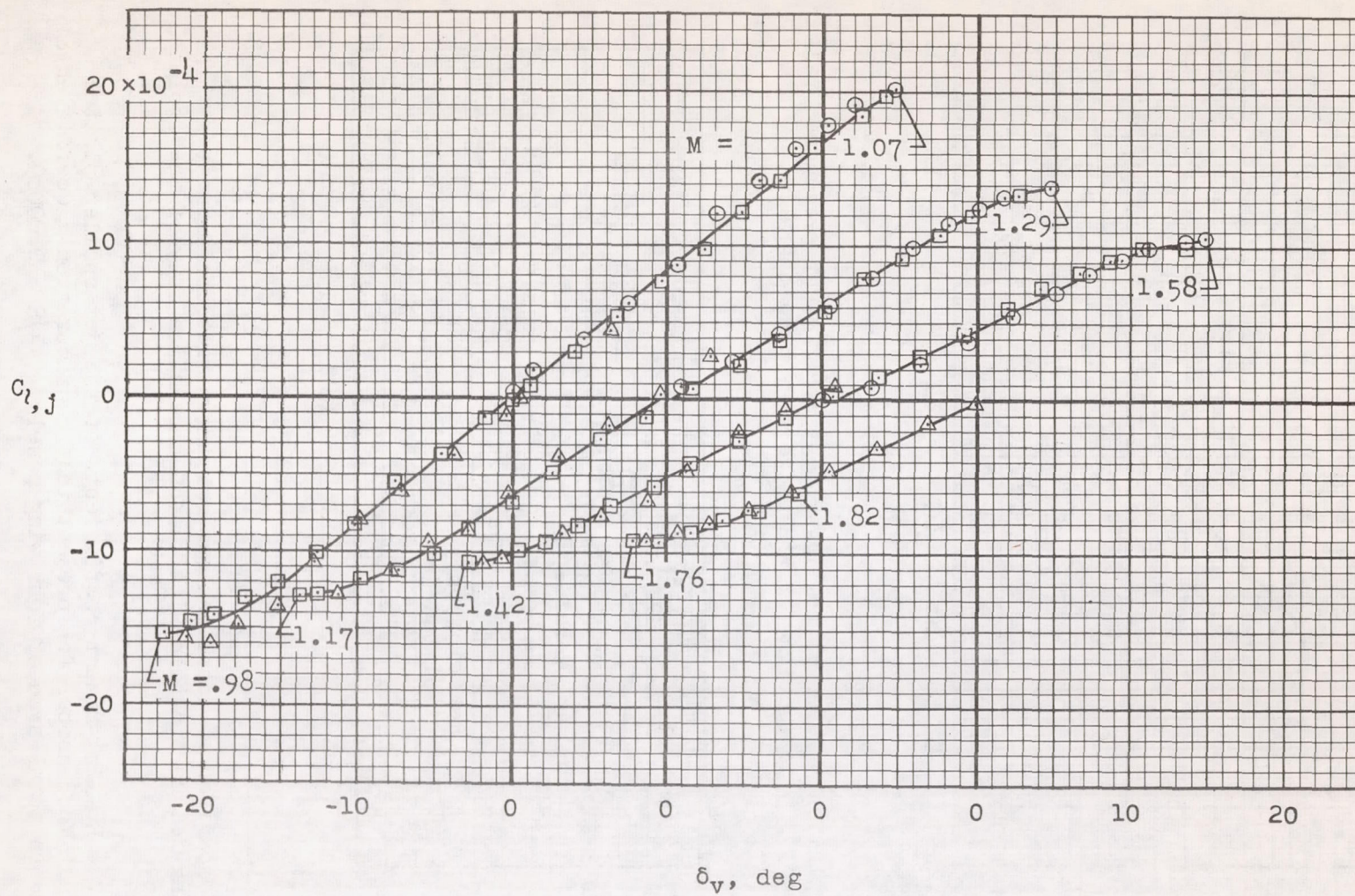


Figure 5.- Histories of roll response, Mach number, and total and static pressures for one pulse of air-jet control valve.



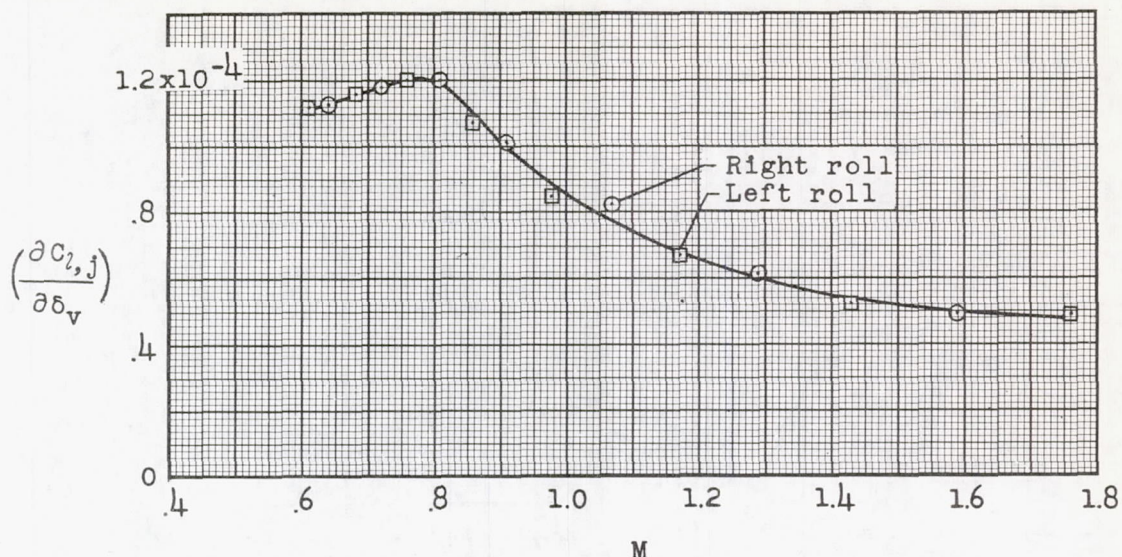
(a) For Mach numbers between 0.59 and 0.92.

Figure 6.- Variation of total rolling-moment coefficient for jet spoiler with valve deflection. Coefficients based on total wing area of four panels. Time increases from right to left in figure.

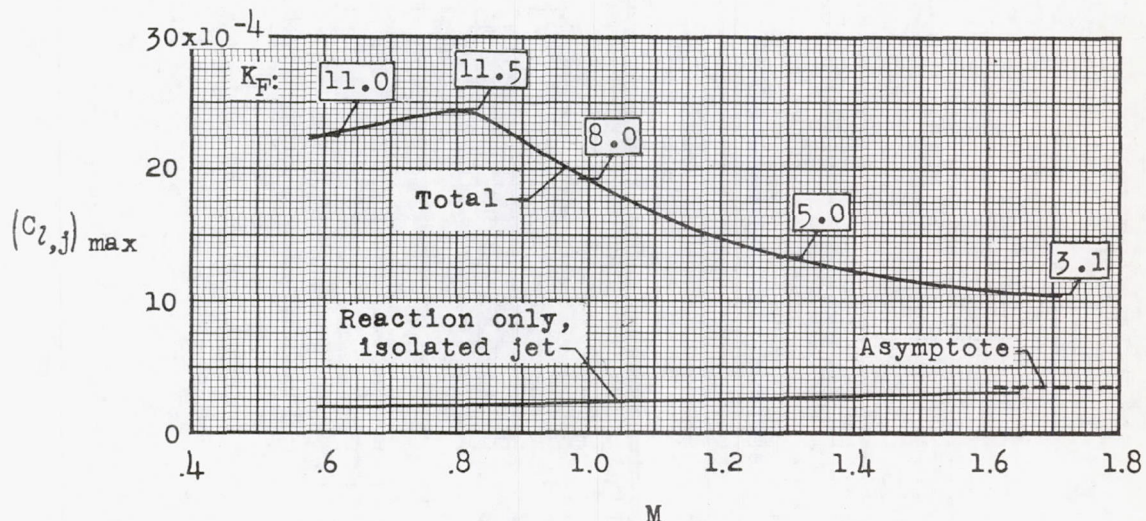


(b) For Mach numbers between 0.98 and 1.82.

Figure 6.- Concluded.



(a) Initial slopes of rolling-moment coefficient per degree valve deflection for the range $-12^\circ < \delta_V < +12^\circ$.



(b) Comparison of total maximum rolling-moment coefficient for the wing-jet combination with that for reaction only of the isolated jet.

Figure 7.- Rolling-moment coefficients of the jet spoiler plotted against Mach number for present test configuration. Coefficients based on total area of four wing panels. $A_j/S = 0.00089$.

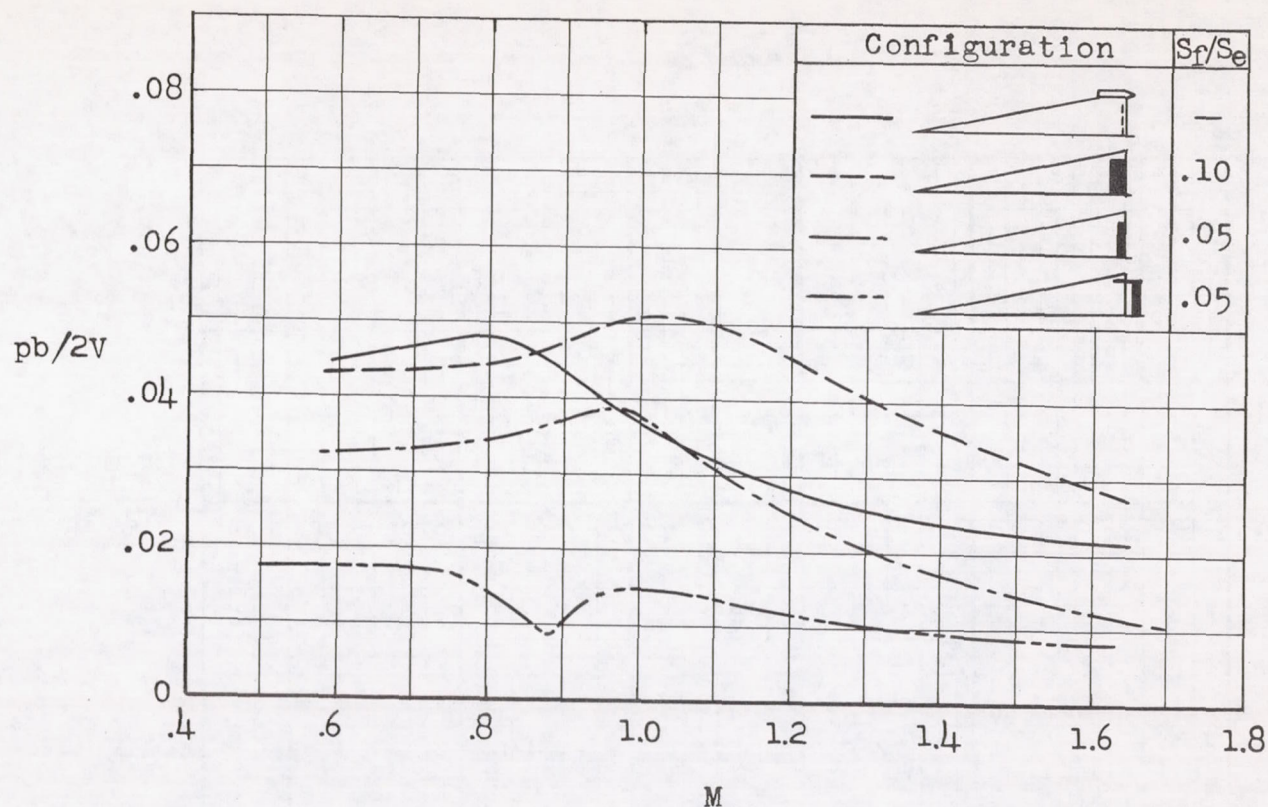


Figure 8.- Comparison of zero-lift rolling effectiveness of the present test jet spoiler with that of conventional deflected surface controls, each deflected 5° . Controls on two of four 80° delta wing panels.

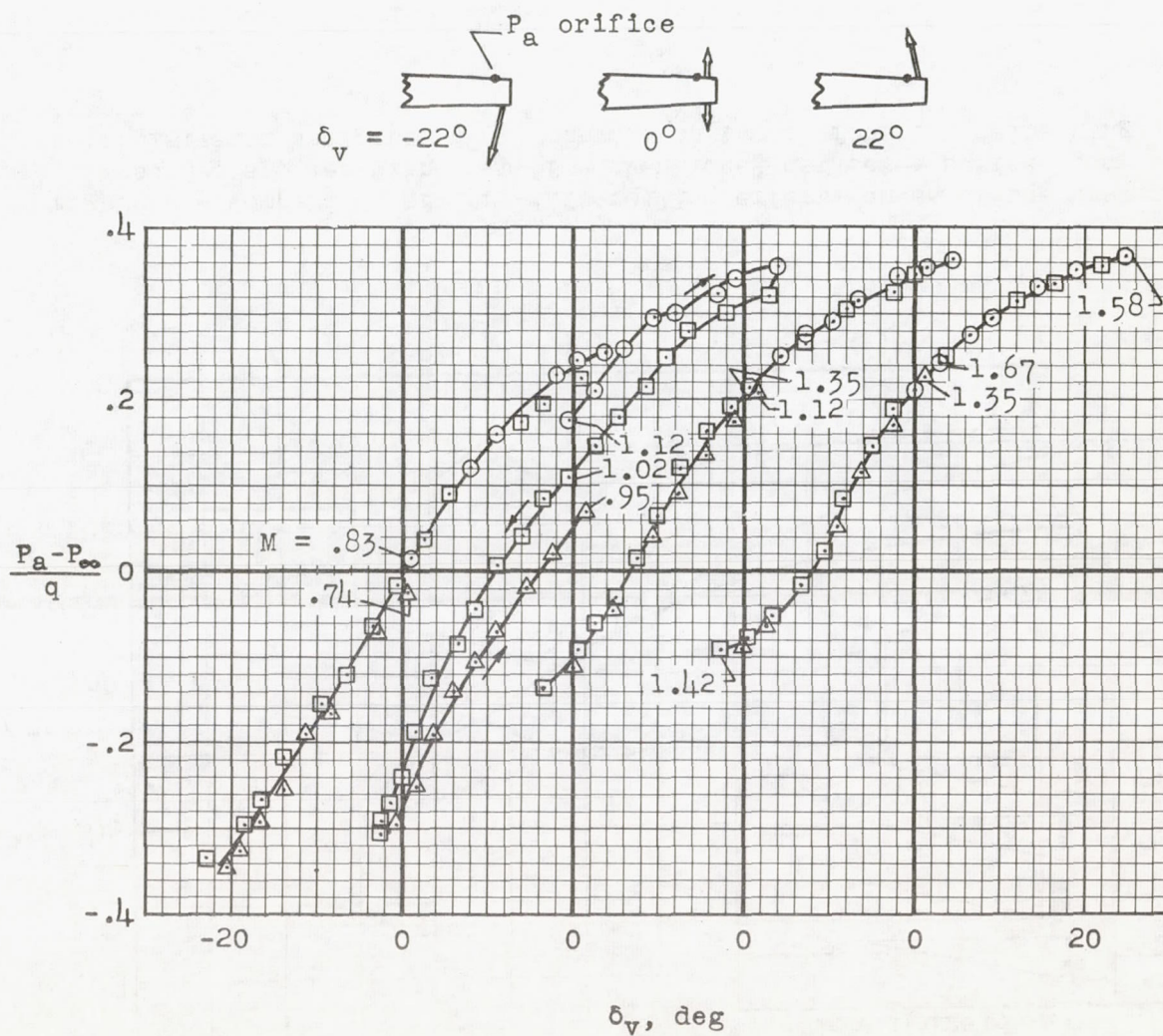


Figure 9.- Variation with valve deflection of upper surface wing static-pressure coefficient just forward of jet at midspan.

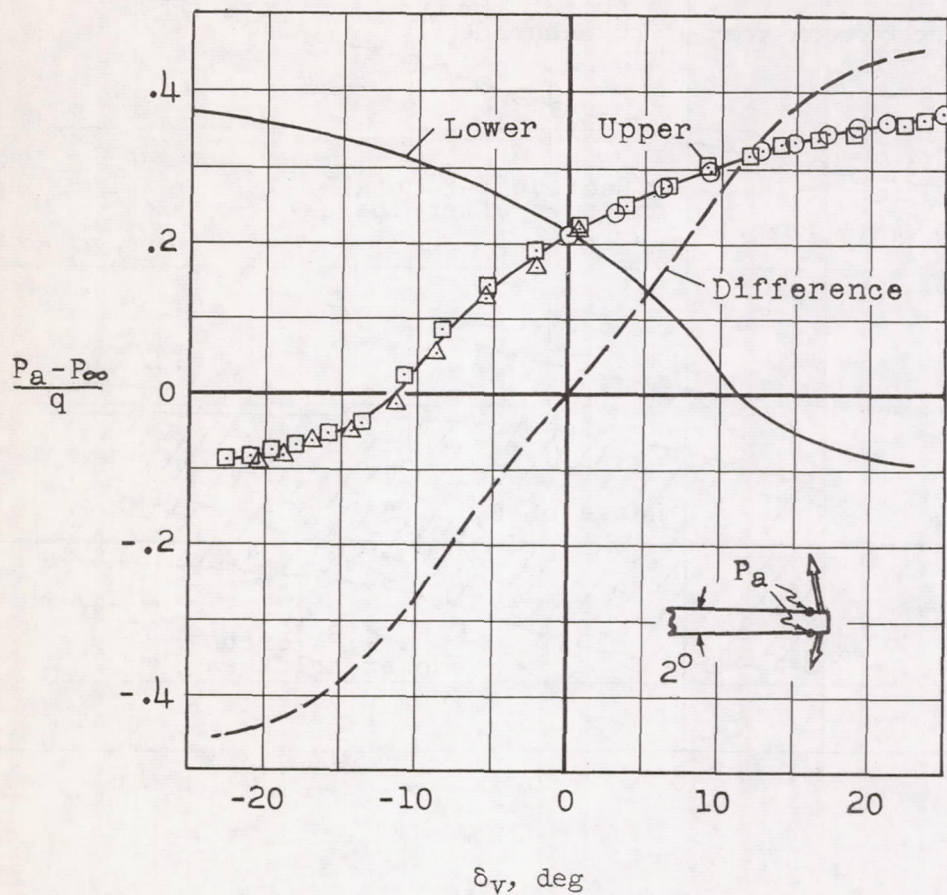


Figure 10.- Variation of pressure difference between upper and lower wing surfaces with valve deflection for the Mach number range between 1.35 and 1.67.

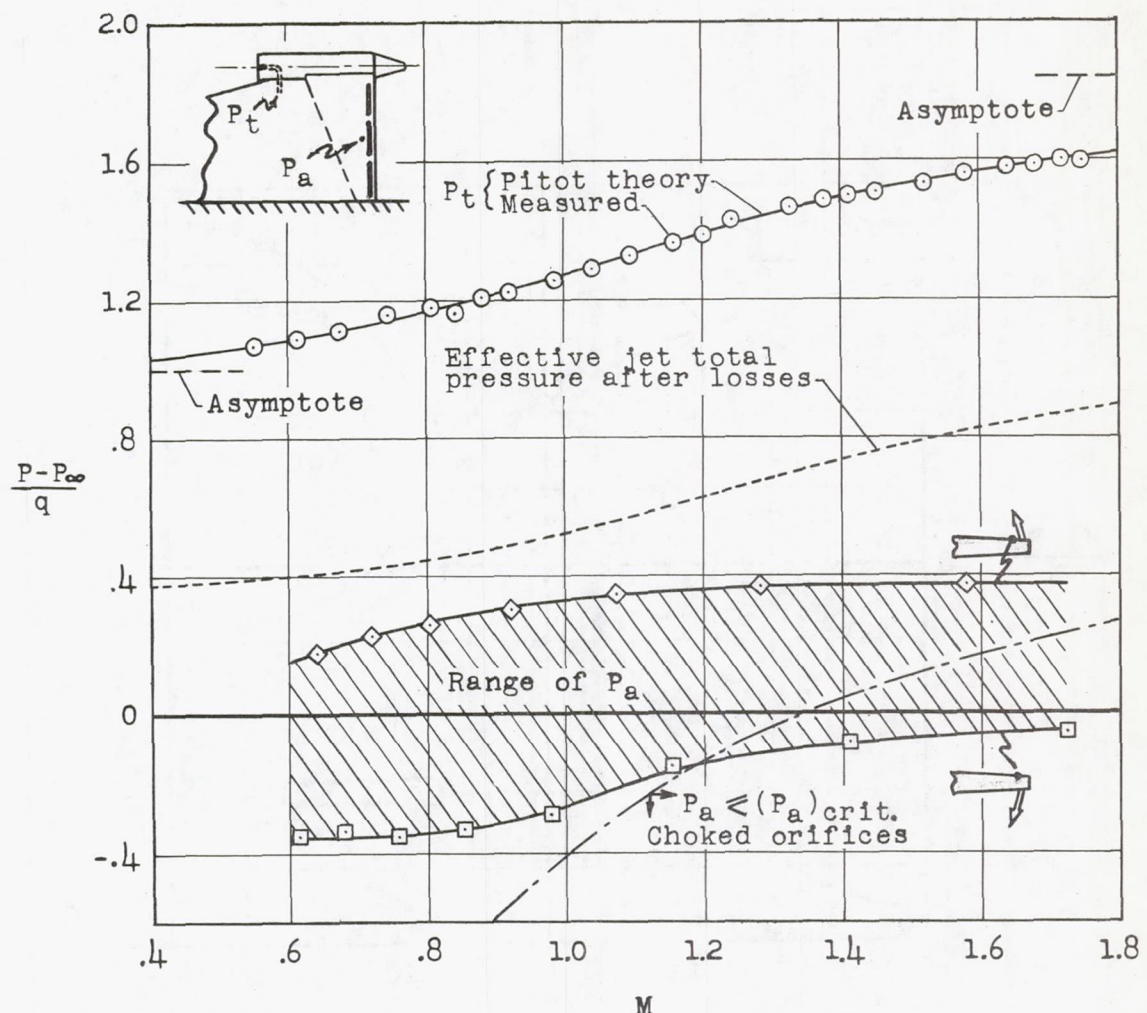


Figure 11.- Variations with Mach number of inlet total-pressure coefficient and range of jet-induced wing-pressure coefficients measured just forward of the jet during control-valve deflection and model roll response.

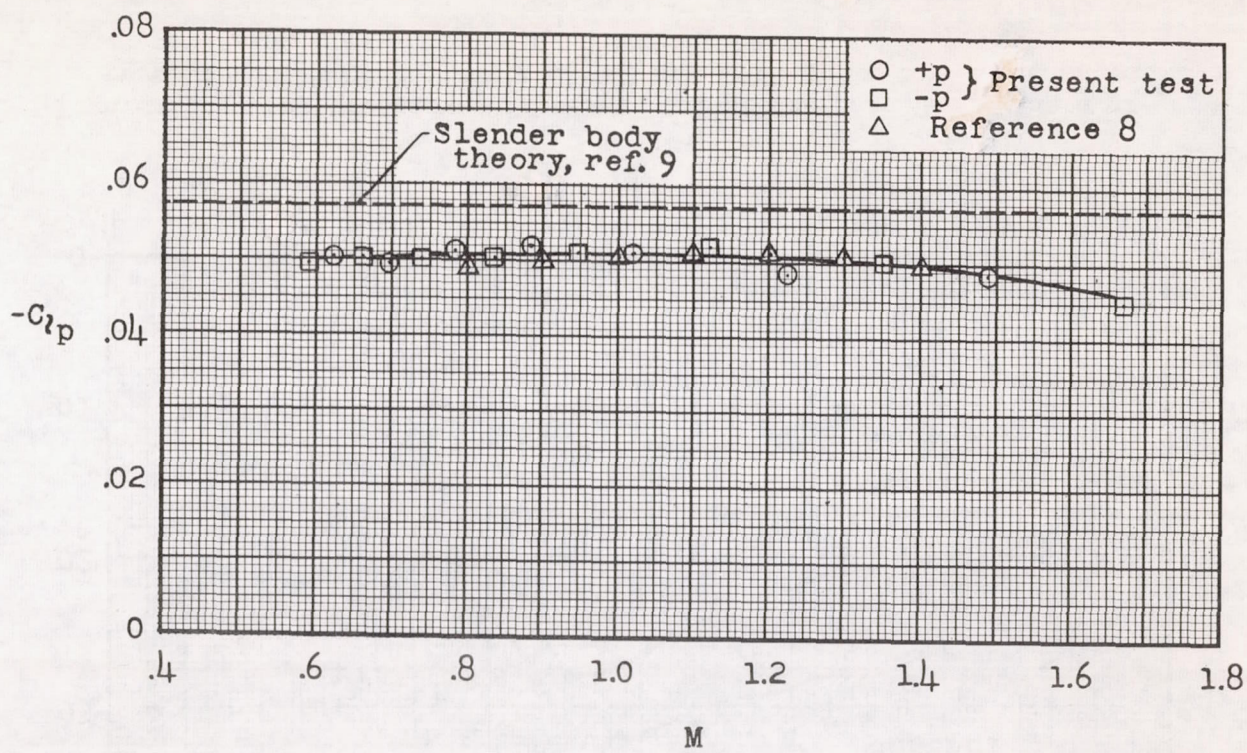


Figure 12.- Variation of damping-in-roll derivative with Mach number for 80° delta-wing-body combination.

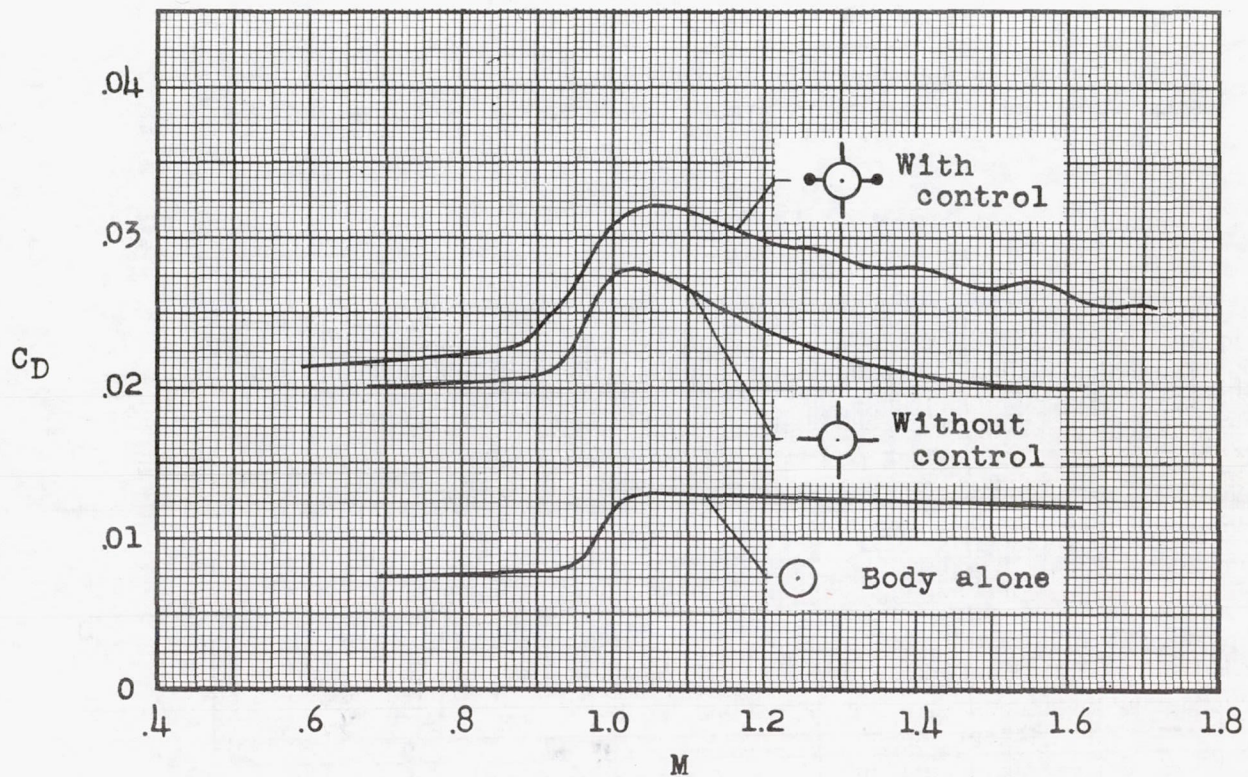


Figure 13.- Drag breakdown of present jet-spoiler model from data of present tests and reference 1. Drag coefficients are based on total exposed wing area.

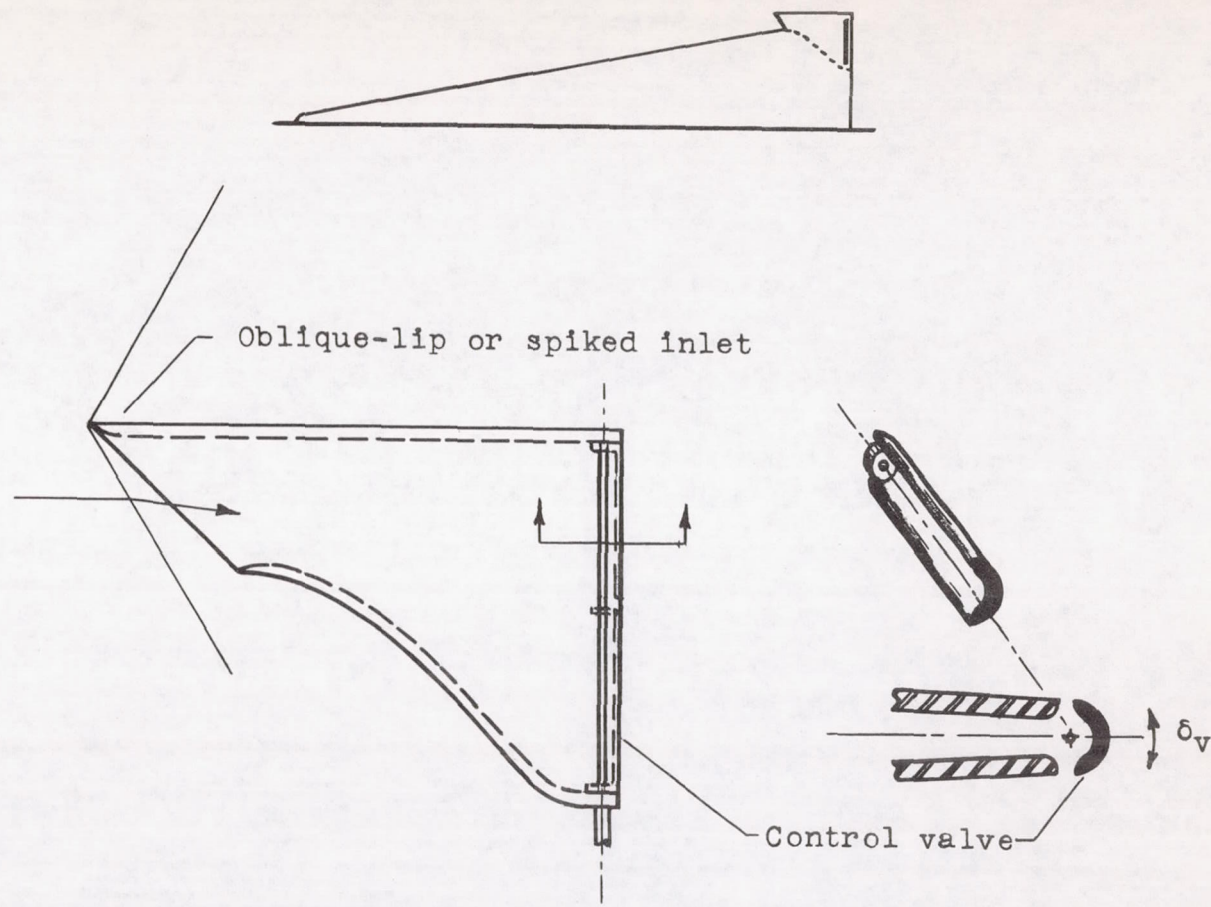


Figure 14.- Possible redesign for improved performance of inlet-jet-spoiler control.